

Entanglement entropy as a probe of topological phase transitions

Manish Kumar,¹ Bharadwaj Vedula,¹ Suhas Gangadharaiah,¹ and Auditya Sharma¹

¹*Department of Physics, Indian Institute of Science Education and Research, Bhopal, Madhya Pradesh 462066, India*

(Dated: August 25, 2025)

Entanglement entropy (EE) provides a powerful probe of quantum phases, yet its role in identifying topological transitions in disordered systems remains underexplored. We introduce an exact EE-based framework that captures topological phase transitions even in the presence of disorder. Specifically, for a class of Su-Schrieffer-Heeger (SSH) model variants, we show that the difference in EE between half-filled and near-half-filled ground states, ΔS^A , vanishes in the topological phase but remains finite in the trivial phase—a direct consequence of edge-state localization. This behavior persists even in the presence of quasiperiodic or binary disorder. Exact phase boundaries, derived from Lyapunov exponents via transfer matrices, agree closely with numerical results from ΔS^A and the topological invariant \mathcal{Q} , with instances where ΔS^A outperforms \mathcal{Q} . Our results highlight EE as a robust diagnostic tool and a potential bridge between quantum information and condensed matter approaches to topological matter.

Introduction— Entanglement entropy (EE) has become a central tool in the study of quantum many-body systems, and quantum phase transitions (QPTs) [1–4]. Defined as the von Neumann entropy of a subsystem, it quantifies the degree of quantum correlations between parts of a system [5]. In conventional systems, QPTs are typically associated with symmetry breaking phenomena [6–8]. However, many exotic phases—such as topological insulators and fractional quantum Hall states—do not fit within this paradigm. Topological phases of matter have been an active field of research in condensed matter physics [9–14] ever since the discovery of the quantum Hall effect [15]. These phases are distinguished by topological invariants [16–21] that remain robust against local perturbations [22–25]. The far-reaching implications of these discoveries [26–29], have inspired work across fields including photonic systems [30–32], ultracold atoms [33–36], and quantum information technologies [37, 38].

Traditionally, topological phase transitions are identified using momentum-space invariants like the winding number [39, 40], and the \mathbb{Z}_2 invariant [41] which rely on translational symmetry and thus break down in disordered systems. To address this, real-space alternatives, such as real space winding numbers [42] and scattering coefficients sensitive to edge-state localization [43, 44], have been developed. Among these, EE has emerged as a uniquely powerful probe. Its non-local character [45] enables detection of topological properties even in many-body states [46, 47] where conventional order parameters fail. In this Letter we provide an exact framework to use many body EE to study topological phase transitions which works even in the presence of disorder.

Despite many studies, a comprehensive understanding of EE across topological phase transitions remains incomplete. While EE’s sensitivity to distinct topological phases is well-established [45–53], the microscopic connection between entanglement patterns and edge-state localization—especially in disordered systems—remains poorly understood. This gap motivates our work, where

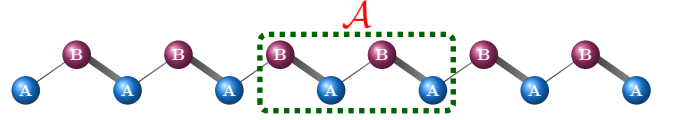


FIG. 1. SSH chain where the green dashed box shows subsystem A composed of a few unit cells deep inside the bulk.

we develop a systematic framework using many particle EE to distinguish topological and trivial phases. For this purpose, we choose the Su-Schrieffer-Heeger (SSH) model [54, 55], which was first introduced to describe both elastic and electronic properties of polyacetylene, a quasi-one-dimensional polymer chain. It is a 1D tight-binding model with non-interacting spinless fermions, and is a standard test-bed for explorations on topological systems. One of the most striking features of the SSH chain is the presence of chiral symmetry protected zero-energy edge states in the topologically non-trivial phase which are robust to local perturbations that preserve the bulk gap and symmetry [56–63].

In this Letter, we propose an EE based approach to study topological phase transitions and demonstrate its robustness by performing an independent transfer matrix based analysis. Specifically, we analytically derive the topological-trivial phase boundaries by calculating the Lyapunov exponent (LE) of edge states in the topological region. While this transfer-matrix-based calculation of the LE has been widely used in the studies of mobility edges in disordered systems [64–68] and Majorana fermionic systems [43, 44, 69], it has not been used in the context of the SSH model. We demonstrate that the phase boundaries obtained from the two methods match perfectly with each other. We further use the topological quantum number \mathcal{Q} [43] which is a well-established quantity that characterizes the presence or absence of Majorana bound states in 1D p-wave superconductors. We also show an example with disorder where EE works better than \mathcal{Q} which exhibits some ambiguity.

Model— The Su–Schrieffer–Heeger (SSH) model [54, 55] describes a one-dimensional dimerized lattice with two sites per unit cell and staggered nearest-neighbour hopping. The Hamiltonian is

$$H = \sum_{n=1}^L \left[t_1 a_n^\dagger b_n + t_2 a_{n+1}^\dagger b_n + \text{H.c.} \right], \quad (1)$$

where a_n^\dagger (b_n^\dagger) creates a particle on sublattice A (B) of the n^{th} unit cell, and L is the total number of unit cells. Since each unit cell contains two sites, the total number of sites is $N = 2L$. The first term represents intracell hopping with strength t_1 , whereas the second corresponds to intercell hopping with strength t_2 . The system is in the trivial phase if $|t_1| > |t_2|$ and in the insulator phase if $|t_1| < |t_2|$. We parameterize t_1 and t_2 with average hopping amplitude t , and dimerization strength λ as

$$\begin{aligned} t_1 &= t - \lambda - \Delta_n, \\ t_2 &= t + \lambda + \Delta_n. \end{aligned} \quad (2)$$

Here, in addition to the clean SSH model ($\Delta_n = 0$ for all n), we study two other cases of disorder in hopping terms; one with quasiperiodic disorder and the other with random binary disorder. In the case of quasiperiodic disorder, $\Delta_n = \delta \cos(2\pi\beta n + \phi)$, where $\beta = (\sqrt{5} - 1)/2$ and ϕ is arbitrarily chosen from a uniform distribution in $[0, 2\pi]$.

In the case of random binary disorder in the hopping strengths, the Δ_n s are drawn from a bimodal probability distribution function [59]

$$\mathcal{P}(\Delta_n) = P \delta(\Delta_n - V_0) + (1 - P) \delta(\Delta_n - V_0 - W), \quad (3)$$

where W is the disorder strength and V_0 is the offset, which we fix at 2. Although random binary disorder in the hopping terms of the SSH model has been explored in earlier studies [59], the specific form considered in Eq. (2) has not been previously analyzed. Next we sketch an analytical approach to determine the topological phase boundary.

Analytical study using transfer matrix—To obtain the boundary of the phase transition we use localization properties of the edge modes. A good quantity to capture the localization behavior is the Lyapunov exponent, which is positive for localized states, and vanishes for delocalized states. In the topological phase, the edge modes are spatially localized on edges, yielding a positive value for the LE γ_0 ; as we approach the phase boundary, the edge modes merge into the bulk and $\gamma_0 \rightarrow 0$. To compute γ_0 , we employ the transfer matrix method. The LE associated with the zero energy mode is defined as

$$\gamma_0 = \lim_{L \rightarrow \infty} \frac{1}{L} \ln \|\mathcal{T}_L\|, \quad (4)$$

where $\mathcal{T}_L = \prod_{n=1}^L T_n$ is the total transfer matrix, and $\|\mathcal{T}_L\|$ represents its norm.

For the clean SSH model, the LE of zero modes is

$$\gamma_0 = \lim_{L \rightarrow \infty} \frac{1}{L} \ln \left| \left(\frac{t_2}{t_1} \right)^L \right| = \ln \left| \frac{t_2}{t_1} \right|. \quad (5)$$

Hence the boundary of the topological phase is $\left| \frac{t_2}{t_1} \right| = 1$. Since t_1 and t_2 are given by Eq. (2), the topological and trivial phases are separated into four quadrants by two lines: $\lambda = 0$, and $t = 0$ (see Fig. 2(a)). In the SSH model with quasiperiodic disorder in the hopping term, we can show that $\gamma_0 > 0$ when $\delta < t + \lambda$ — this regime exhibits localized zero edge modes and hence corresponds to a topological insulating phase. The LE tends to zero at the topological phase boundary given by $\delta = t + \lambda$. This analytical expression is consistent with numerical studies with quasiperiodic modulation in the hopping amplitudes (see Fig. 2 and Ref. [57]). In the case of random binary disorder, the phase transition boundary (where $\gamma \rightarrow 0$) is given by

$$\left| \left(\frac{u}{v} \right)^P \left(\frac{u - W}{v + W} \right)^{1-P} \right| = 1, \quad (6)$$

with $u = t + \lambda + 2$ and $v = t - \lambda - 2$. The detailed derivation of the above results is shown in the supplementary material [70].

Entanglement Entropy—We next investigate the phase transition between topological and trivial insulating states using the entanglement entropy as a diagnostic measure. For this we consider the correlation matrix $C_{ij} = \langle c_i^\dagger c_j \rangle$ and calculate the EE of the subsystem \mathcal{A} as [71–73]

$$S^{\mathcal{A}} = - \sum_k [\lambda_k \ln \lambda_k + (1 - \lambda_k) \ln(1 - \lambda_k)] \quad (7)$$

where λ_k are the eigenvalues of the subsystem correlation matrix.

We show that the EE of the many-body ground state serves as an effective probe to detect the quantum phase transition between the topological and the trivial insulating phases. To use EE as a diagnostic tool, it is crucial to define the subsystem appropriately. Choosing region \mathcal{A} as a few unit cells deep in the bulk (Fig. 1), and the rest as \mathcal{B} , proves to be an effective choice. We then compute the EE difference between the ground state at half-filling and one more than half filling, defined as

$$\Delta S^{\mathcal{A}} = |S_{\text{hf}}^{\mathcal{A}} - S_{\text{hf}+1}^{\mathcal{A}}|. \quad (8)$$

This quantity provides a sharp and robust signature of the topological phase transition. Considering the difference with respect to a state with one particle less than half-filling ($|S_{\text{hf}}^{\mathcal{A}} - S_{\text{hf}-1}^{\mathcal{A}}|$) also yields similar results, though we focus on the added-particle case in this work.

In the clean SSH model, the t – λ phase diagram obtained from $\Delta S^{\mathcal{A}}$ (Fig. 2(a)) yields $\Delta S^{\mathcal{A}} = 0$ in the topological phase while it is non-zero in the trivial phase. We

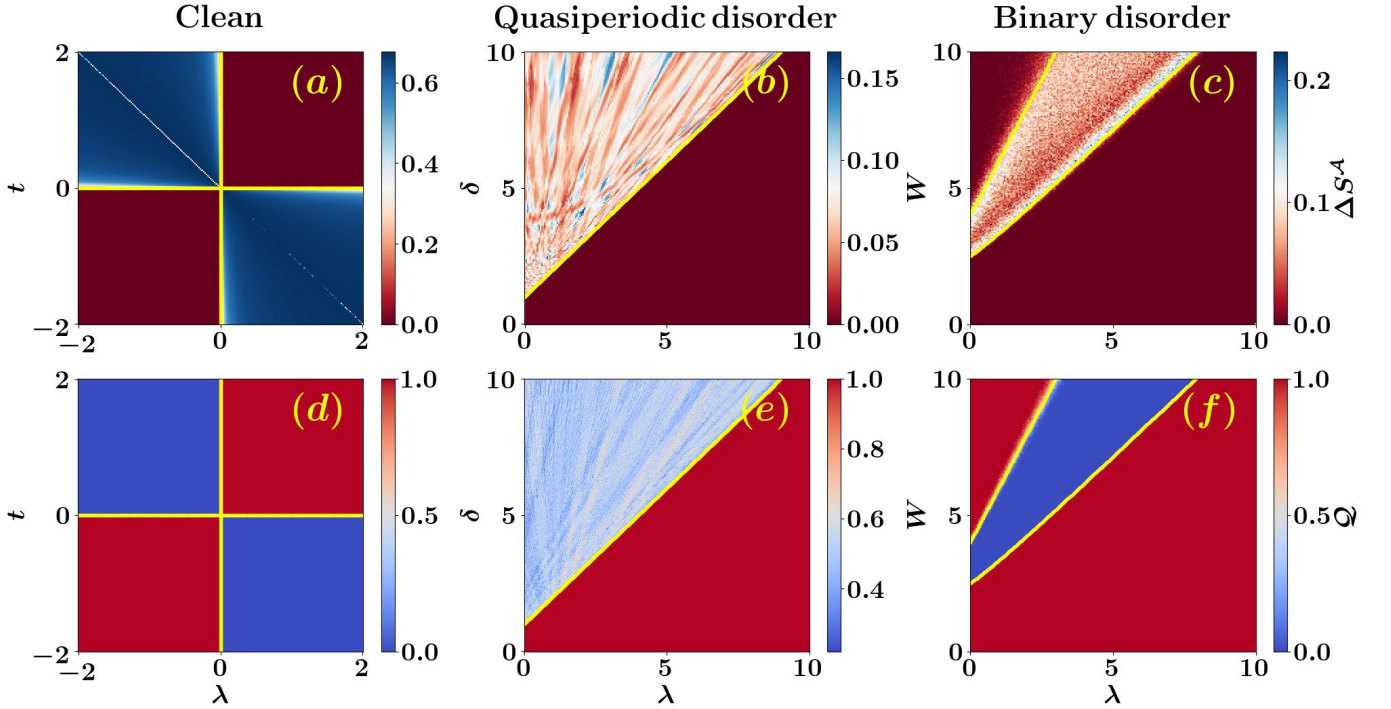


FIG. 2. Phase diagrams of the SSH model variants. In (a)–(c) the color scale denotes $\Delta S^A = |S_{\text{hf}}^A - S_{\text{hf}+1}^A|$ with $\text{hf} = N/2$, $N = 400$, and the subsystem size $N_A = 50$. In (d)–(f) the color scale denotes topological quantum number Q for $N = 2000$. All results are averaged over 100 realizations with $t = 1$. Yellow curves mark analytical phase boundaries.

further apply this analysis to the SSH model with both quasiperiodic and random binary disorder in the hopping term. In the quasiperiodic case, the phase boundary is given by $\delta = t + \lambda$ (see Fig. 2(b)) while in the random binary case with $P = 1/2$ and $t = 1$, the transition line follows from Eq. (6) (see (Fig. 2(c))). For both these cases, ΔS^A vanishes in the topological phase and is nonzero in the trivial phase, demonstrating its robustness as a detector of topological phases. Additional data for other values of t and P are shown in the supplementary material [70].

Occupation number—To understand the behavior of EE, we examine the spatial distribution of the added particle by analyzing the site occupations of the full system. The site occupations correspond to the diagonal elements of the full system’s correlation matrix C . In particular, we consider the change in site occupations defined as

$$\Delta\Omega(i) = |\Omega_{\text{hf}}(i) - \Omega_{\text{hf}+1}(i)|, \quad (9)$$

where $\Omega(i)$ denotes the occupation of the i^{th} site, and $\Delta\Omega$ reveals the occupation of the additional particle introduced beyond half-filling. The spatial profile of $\Delta\Omega$ for the quasiperiodic disorder case and the random binary disorder case are shown for in Fig. 3(a) and 3(b) respectively. In both the cases, within the topological phase (green curve), $\Delta\Omega$ is nonzero only at the edges, indicating that the added particle is edge-localized and does not enter subsystem \mathcal{A} , therefore EE does not ex-

hibit any change. However, in the trivial phase (brown curve), the particle spreads into both \mathcal{A} and \mathcal{B} , contributing to EE and resulting in a nonzero ΔS^A . This pattern is consistent across all cases, regardless of the type of disorder.

Topological quantum number—To contrast our results obtained using EE, we employ the topological quantum number Q , which has been shown to be a useful quantity to distinguish the topological phase from the trivial phase [43, 44]. The topological quantum number is defined as $Q = \frac{1}{2}(1 - Q')$, where $Q' = \text{sign}(r) \in \{-1, 1\}$ and r is the reflection matrix. For a single SSH chain, the reflection matrix r is a scalar:

$$r = \frac{1 - X^2}{1 + X^2}, \quad (10)$$

where $X = (-1)^{N/2} \prod_{n=1}^{N/2} \frac{t_{2,n}}{t_{1,n}}$. For the trivial phase, $Q = 0$ (no edge modes) while in the topological phase, $Q = 1$ due to the presence of a pair of zero-energy edge modes [43]. To corroborate the results from ΔS^A , we present phase diagrams for all three cases in Figs. 2(d–f). For the clean SSH model (Fig. 2(d)) and the binary random disorder model (Fig. 2(f)), our results show the expected behavior, i.e., $Q = 1$ in the topological regime and $Q = 0$ in the trivial regime. The analytically calculated boundaries, shown as yellow lines, match precisely with the numerical results. This confirms that ΔS^A effectively captures the topological phase transition.

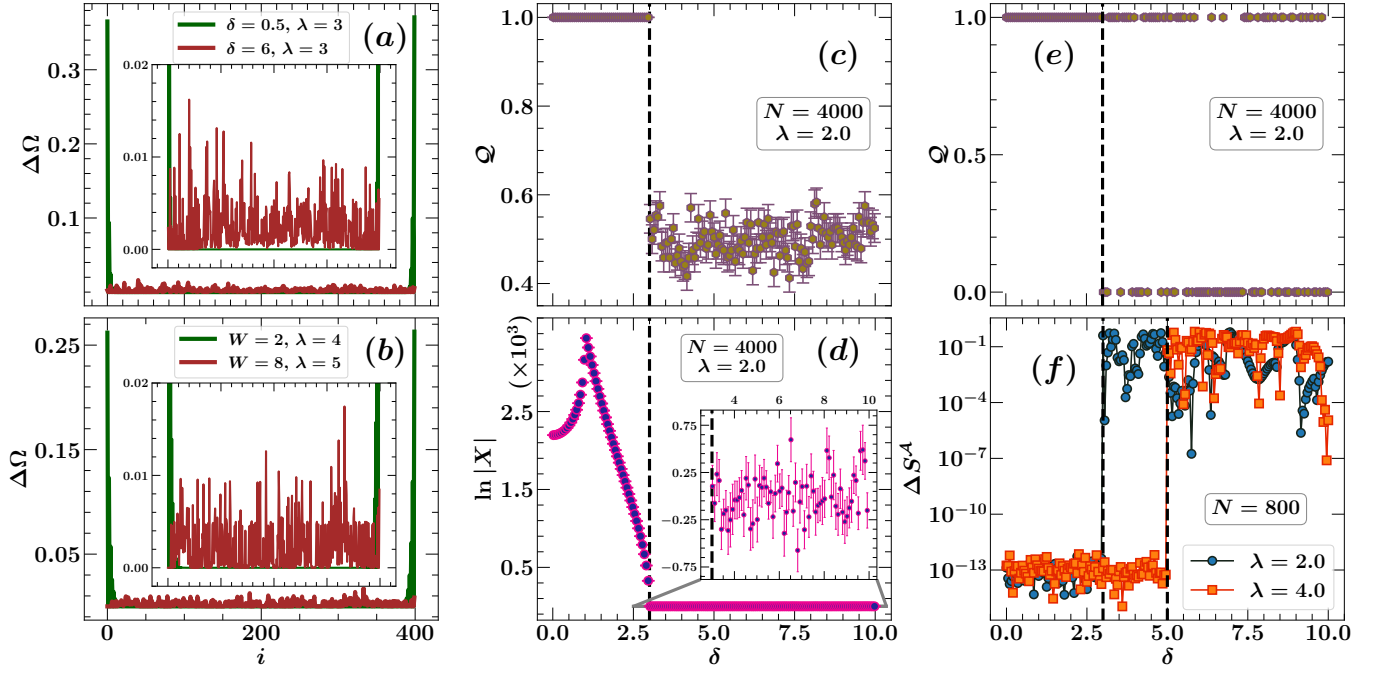


FIG. 3. Distinguishing topological and trivial phases via occupation number, topological invariants, and entanglement entropy. (a,b) Spatial distribution of the change in occupation number $\Delta\Omega = |\Omega_{\text{hf}} - \Omega_{\text{hf}+1}|$ for (a) quasiperiodic and (b) binary disorder, averaged over 100 configurations. The added particle localizes at the edges (green, topological) or delocalizes into the bulk (brown, trivial). Insets: zoomed in version of the main figure shows that $\Delta\Omega$ remains finite within the bulk subsystem \mathcal{A} in the trivial phase. (c,d) For the quasiperiodic model, (c) the topological quantum number Q and (d) the quantity $\ln|X|$ versus disorder strength δ , averaged over 480 configurations. (e,f) Direct comparison of Q with the entanglement entropy $\Delta S^{\mathcal{A}}$ for a single realization of the quasiperiodic model. Black dashed lines mark the analytical phase boundary at $\delta = t + \lambda$. We find misleading instances where $Q = 1$ even in the trivial region. In contrast $\Delta S^{\mathcal{A}}$ provides a sharp and reliable distinction between the two phases. System sizes and specific parameters are indicated in the figure panels ($t = 1$ in all cases).

For the case of quasiperiodic disorder, Fig. 2(e) shows $Q = 1$ in the entire topological regime. However, in the trivial regime, Q displays deviation from expected behavior, i.e., it acquires non-zero values. In particular, for $\lambda = 2$, it converges to approximately 0.5 in the trivial regime when averaged over multiple values of ϕ (see Fig. 3(c)). Next, we delve into the quantity $Q' = \text{sign}(1 - X^2) = -\text{sign}(\log|X|)$, which changes sign at the phase transition. Figure 3(d) shows that in the topological regime, $\log|X| > 0$ but in the trivial regime, $\log|X|$ fluctuates around zero, resulting in an average $Q \approx 0.5$. To further understand this behavior we study Q for a single realization.

Comparison between Q and $\Delta S^{\mathcal{A}}$ —We now compare Q and $\Delta S^{\mathcal{A}}$ for a single value of ϕ . In Fig. 3(e), we plot Q as a function of δ for $\lambda = 2$. While in the entire topological region ($\delta < t + \lambda$) $Q = 1$, it turns out that even within the trivial region ($\delta > t + \lambda$) we find instances where $Q = 1$, falsely suggesting topological insulating behavior. This highlights the inability of Q to sharply detect the topological transition. In contrast our proposed diagnostic $\Delta S^{\mathcal{A}}$ remains finite in the trivial phase and vanishes in the topological phase, thereby providing a sharp and reliable distinction between the two, as

shown in Fig. 3(f). Extended phase diagrams over the (δ, λ) plane, presented in Sec. IV of the supplementary material [70], further corroborate this conclusion.

Summary and Outlook—In this Letter, we demonstrate that entanglement entropy can serve as an effective probe for detecting topological phase transitions in the Su-Schrieffer-Heeger (SSH) model and its disordered variants. We study the clean SSH model as well as two extensions incorporating quasiperiodic and random binary disorder in the hopping terms. We show that the EE of the many-body ground state at half-filling, and at one particle above half-filling remain identical in the topological regime, while they differ in the trivial regime. This distinction arises because in the topological regime, the added particle localizes at the edges and does not contribute to the entanglement of the bulk subsystem. To substantiate these results, we employ an analytical approach based on the Lyapunov exponent, computed through the transfer matrix method, to determine the phase boundaries. This method is simple and applicable to systems with disorder. We observe excellent agreement between the LE-based analytical results and numerical results across all models. To further validate our findings, we compare with the topological invariant Q ,

which matches our results in the clean and random binary cases. However, for the model with the quasiperiodic disorder, \mathcal{Q} shows ambiguity in the trivial regime. Comparing with the EE-based measure ΔS^A , we find the latter to be more robust, even for a single disorder realization. Our work thus presents a unified framework combining EE and LE to detect topological phases in disordered 1D systems.

One dimensional systems host only two edge modes; higher-dimensional topological insulators (e.g., 2D Chern insulators or 3D \mathbb{Z}_2 topological insulators) exhibit richer edge/surface state structures. Extending this EE based diagnostic to higher dimensions could offer deeper insights into the link between topology and entanglement. Since topological phases exhibit long-range entanglement [47], our work contributes to the growing field of quantum information science and condensed matter physics. This positions ΔS^A as a potential universal tool for characterizing topological matter across dimensions.

Acknowledgments—We thank Ivan M. Khaymovich for valuable discussions. We are grateful to the High Performance Computing (HPC) facility at IISER Bhopal, where some calculations in this project were run. M.K is grateful to the Council of Scientific and Industrial Research (CSIR), India, for his PhD fellowship.

-
- [1] A. Osterloh, L. Amico, G. Falci, and R. Fazio, Scaling of entanglement close to a quantum phase transition, *Nature* **416**, 608 (2002).
 - [2] G. Vidal, J. I. Latorre, E. Rico, and A. Kitaev, Entanglement in quantum critical phenomena, *Phys. Rev. Lett.* **90**, 227902 (2003).
 - [3] T. J. Osborne and M. A. Nielsen, Entanglement in a simple quantum phase transition, *Phys. Rev. A* **66**, 032110 (2002).
 - [4] J. Eisert, M. Cramer, and M. B. Plenio, Colloquium: Area laws for the entanglement entropy, *Rev. Mod. Phys.* **82**, 277 (2010).
 - [5] C. H. Bennett, H. J. Bernstein, S. Popescu, and B. Schumacher, Concentrating partial entanglement by local operations, *Phys. Rev. A* **53**, 2046 (1996).
 - [6] L. D. Landau, On the theory of phase transitions, *Zh. Eksp. Teor. Fiz.* **7**, 19 (1937).
 - [7] A. J. Beekman, L. Rademaker, and J. van Wezel, An introduction to spontaneous symmetry breaking, *SciPost Phys. Lect. Notes*, 11 (2019).
 - [8] L. D. Landau, E. M. Lifshitz, E. M. Lifshits, and L. P. Pitaevskii, *Statistical Physics: Theory of the Condensed State*, Vol. 9 (Butterworth-Heinemann, London, 1980).
 - [9] M. Z. Hasan and C. L. Kane, Colloquium: Topological insulators, *Rev. Mod. Phys.* **82**, 3045 (2010).
 - [10] X.-L. Qi and S.-C. Zhang, Topological insulators and superconductors, *Rev. Mod. Phys.* **83**, 1057 (2011).
 - [11] J. E. Moore, The birth of topological insulators, *Nature* **464**, 194 (2010).
 - [12] L. Fu and C. L. Kane, Topological insulators with inversion symmetry, *Phys. Rev. B* **76**, 045302 (2007).
 - [13] B. A. Bernevig, *Topological Insulators and Topological Superconductors* (Princeton University Press, Princeton, 2013).
 - [14] J. K. Asbóth, L. Oroszlány, and A. Pályi, *A Short Course on Topological Insulators* (Springer International Publishing, 2016).
 - [15] K. v. Klitzing, G. Dorda, and M. Pepper, New method for high-accuracy determination of the fine-structure constant based on quantized hall resistance, *Phys. Rev. Lett.* **45**, 494 (1980).
 - [16] J. E. Moore and L. Balents, Topological invariants of time-reversal-invariant band structures, *Phys. Rev. B* **75**, 121306 (2007).
 - [17] D. N. Sheng, Z. Y. Weng, L. Sheng, and F. D. M. Haldane, Quantum spin-hall effect and topologically invariant chern numbers, *Phys. Rev. Lett.* **97**, 036808 (2006).
 - [18] T. Fukui and Y. Hatsugai, Topological aspects of the quantum spin-hall effect in graphene: \mathbb{Z}_2 topological order and spin chern number, *Phys. Rev. B* **75**, 121403 (2007).
 - [19] C. L. Kane and E. J. Mele, \mathbb{Z}_2 topological order and the quantum spin hall effect, *Phys. Rev. Lett.* **95**, 146802 (2005).
 - [20] L. Fu and C. L. Kane, Time reversal polarization and a \mathbb{Z}_2 adiabatic spin pump, *Phys. Rev. B* **74**, 195312 (2006).
 - [21] R. Roy, \mathbb{Z}_2 classification of quantum spin hall systems: An approach using time-reversal invariance, *Phys. Rev. B* **79**, 195321 (2009).
 - [22] E. Prodan, Robustness of the spin-cheren number, *Phys. Rev. B* **80**, 125327 (2009).
 - [23] B. Leung and E. Prodan, Effect of strong disorder in a three-dimensional topological insulator: Phase diagram and maps of the F_2 invariant, *Phys. Rev. B* **85**, 205136 (2012).
 - [24] Z. Wang and S.-C. Zhang, Simplified topological invariants for interacting insulators, *Phys. Rev. X* **2**, 031008 (2012).
 - [25] B. Pérez-González, M. Bello, A. Gómez-León, and G. Platero, Interplay between long-range hopping and disorder in topological systems, *Phys. Rev. B* **99**, 035146 (2019).
 - [26] L. Li and S. Chen, Characterization of topological phase transitions via topological properties of transition points, *Phys. Rev. B* **92**, 085118 (2015).
 - [27] C.-K. Chiu, J. C. Y. Teo, A. P. Schnyder, and S. Ryu, Classification of topological quantum matter with symmetries, *Rev. Mod. Phys.* **88**, 035005 (2016).
 - [28] X.-G. Wen, Colloquium: Zoo of quantum-topological phases of matter, *Rev. Mod. Phys.* **89**, 041004 (2017).
 - [29] B. J. Wieder, B. Bradlyn, J. Cano, Z. Wang, M. G. Vergniory, L. Elcoro, A. A. Soluyanov, C. Felser, T. Neupert, N. Regnault, and B. A. Bernevig, Topological materials discovery from crystal symmetry, *Nature Reviews Materials* **7**, 196 (2022).
 - [30] K. L. Hur, L. Henriët, A. Petrescu, K. Plekhanov, G. Roux, and M. Schiró, Many-body quantum electrodynamics networks: Non-equilibrium condensed matter physics with light, *Comptes Rendus. Physique* **17**, 808 (2016).
 - [31] L. Lu, J. D. Joannopoulos, and M. Soljačić, Topological photonics, *Nature Photonics* **8**, 821 (2014).
 - [32] T. Ozawa, H. M. Price, A. Amo, N. Goldman, M. Hafezi, L. Lu, M. C. Rechtsman, D. Schuster, J. Simon, O. Zilberberg, and I. Carusotto, Topological photonics, *Rev.*

- Mod. Phys. **91**, 015006 (2019).
- [33] D. Zhang, M. Long, L. Cui, J. Xiao, and C. Pan, Perfect spin-filtering and switching functions in zigzag silicene nanoribbons with hydrogen modification, *Organic Electronics* **62**, 253 (2018).
 - [34] V. Galitski and I. B. Spielman, Spin-orbit coupling in quantum gases, *Nature* **494**, 49 (2013).
 - [35] N. R. Cooper, J. Dalibard, and I. B. Spielman, Topological bands for ultracold atoms, *Rev. Mod. Phys.* **91**, 015005 (2019).
 - [36] N. Goldman, J. C. Budich, and P. Zoller, Topological quantum matter with ultracold gases in optical lattices, *Nature Physics* **12**, 639 (2016).
 - [37] G. Vidal, Efficient classical simulation of slightly entangled quantum computations, *Phys. Rev. Lett.* **91**, 147902 (2003).
 - [38] R. Pawlak, S. Hoffman, J. Klinovaja, D. Loss, and E. Meyer, Majorana fermions in magnetic chains, *Progress in Particle and Nuclear Physics* **107**, 1 (2019).
 - [39] L. Li, C. Yang, and S. Chen, Winding numbers of phase transition points for one-dimensional topological systems, *Europhysics Letters* **112**, 10004 (2015).
 - [40] R. K. Malakar and A. K. Ghosh, Engineering topological phases of any winding and chern numbers in extended su-schrieffer-heeger models, *Journal of Physics: Condensed Matter* **35**, 335401 (2023).
 - [41] M. G. Yamada, Topological Z_2 invariant in kitaev spin liquids: Classification of gapped spin liquids beyond projective symmetry group, *Phys. Rev. Res.* **3**, L012001 (2021).
 - [42] I. Mondragon-Shem, T. L. Hughes, J. Song, and E. Prodan, Topological criticality in the chiral-symmetric aiii class at strong disorder, *Phys. Rev. Lett.* **113**, 046802 (2014).
 - [43] I. C. Fulga, F. Hassler, A. R. Akhmerov, and C. W. J. Beenakker, Scattering formula for the topological quantum number of a disordered multimode wire, *Phys. Rev. B* **83**, 155429 (2011).
 - [44] P. Zhang and F. Nori, Majorana bound states in a disordered quantum dot chain, *New Journal of Physics* **18**, 043033 (2016).
 - [45] N. Ahmadi, J. Abouie, and D. Baeriswyl, Topological and nontopological features of generalized su-schrieffer-heeger models, *Phys. Rev. B* **101**, 195117 (2020).
 - [46] R. Nehra, D. S. Bhakuni, S. Gangadharaiah, and A. Sharma, Many-body entanglement in a topological chiral ladder, *Phys. Rev. B* **98**, 045120 (2018).
 - [47] B. Zeng, X. Chen, D.-L. Zhou, and X.-G. Wen, *Quantum information meets quantum matter – from quantum entanglement to topological phase in many-body systems* (2018), [arXiv:1508.02595 \[cond-mat.str-el\]](https://arxiv.org/abs/1508.02595).
 - [48] A. Hamma, W. Zhang, S. Haas, and D. A. Lidar, Entanglement, fidelity, and topological entropy in a quantum phase transition to topological order, *Phys. Rev. B* **77**, 155111 (2008).
 - [49] T. P. Oliveira and P. D. Sacramento, Entanglement modes and topological phase transitions in superconductors, *Phys. Rev. B* **89**, 094512 (2014).
 - [50] H.-C. Jiang, Z. Wang, and L. Balents, Identifying topological order by entanglement entropy, *Nature Physics* **8**, 902 (2012).
 - [51] T. Masłowski and N. Sedlmayr, Quasiperiodic dynamical quantum phase transitions in multiband topological insulators and connections with entanglement entropy and fidelity susceptibility, *Phys. Rev. B* **101**, 014301 (2020).
 - [52] C. Castelnovo and C. Chamon, Quantum topological phase transition at the microscopic level, *Phys. Rev. B* **77**, 054433 (2008).
 - [53] T. Grover, A. M. Turner, and A. Vishwanath, Entanglement entropy of gapped phases and topological order in three dimensions, *Phys. Rev. B* **84**, 195120 (2011).
 - [54] W. P. Su, J. R. Schrieffer, and A. J. Heeger, Solitons in polyacetylene, *Phys. Rev. Lett.* **42**, 1698 (1979).
 - [55] W. P. Su, J. R. Schrieffer, and A. J. Heeger, Soliton excitations in polyacetylene, *Phys. Rev. B* **22**, 2099 (1980).
 - [56] L. Li, Z. Xu, and S. Chen, Topological phases of generalized su-schrieffer-heeger models, *Phys. Rev. B* **89**, 085111 (2014).
 - [57] T. Liu and H. Guo, Topological phase transition in the quasiperiodic disordered su-schrieffer-heeger chain, *Physics Letters A* **382**, 3287 (2018).
 - [58] A. Sinha, T. Shit, A. Tatarwal, D. Sen, and S. Mukherjee, Probing the topological anderson transition in quasiperiodic photonic lattices via chiral displacement and wavelength tuning, *Phys. Rev. A* **112**, 013512 (2025).
 - [59] S.-N. Liu, G.-Q. Zhang, L.-Z. Tang, and D.-W. Zhang, Topological anderson insulators induced by random binary disorders, *Physics Letters A* **431**, 128004 (2022).
 - [60] S. Mandal and S. Kar, Topological solitons in a su-schrieffer-heeger chain with periodic hopping modulation, domain wall, and disorder, *Phys. Rev. B* **109**, 195124 (2024).
 - [61] S. Li, M. Liu, F. Li, and B. Liu, Topological phase transition of the extended non-hermitian su-schrieffer-heeger model, *Physica Scripta* **96**, 015402 (2020).
 - [62] A. Nava, G. Campagnano, P. Sodano, and D. Giuliano, Lindblad master equation approach to the topological phase transition in the disordered su-schrieffer-heeger model, *Phys. Rev. B* **107**, 035113 (2023).
 - [63] Z.-S. Xu, J. Gao, A. Iovan, I. M. Khaymovich, V. Zwiller, and A. W. Elshaari, Observation of reentrant metal-insulator transition in a random-dimer disordered ssh lattice, *npj Nanophotonics* **1**, 8 (2024).
 - [64] Y. Wang, X. Xia, L. Zhang, H. Yao, S. Chen, J. You, Q. Zhou, and X.-J. Liu, One-dimensional quasiperiodic mosaic lattice with exact mobility edges, *Phys. Rev. Lett.* **125**, 196604 (2020).
 - [65] X. Cai and Y.-C. Yu, Exact mobility edges in quasiperiodic systems without self-duality, *Journal of Physics: Condensed Matter* **35**, 035602 (2022).
 - [66] X.-C. Zhou, Y. Wang, T.-F. J. Poon, Q. Zhou, and X.-J. Liu, Exact new mobility edges between critical and localized states, *Phys. Rev. Lett.* **131**, 176401 (2023).
 - [67] Z. Wang, Y. Zhang, L. Wang, and S. Chen, Engineering mobility in quasiperiodic lattices with exact mobility edges, *Phys. Rev. B* **108**, 174202 (2023).
 - [68] Y. Wang, X. Xia, Y. Wang, Z. Zheng, and X.-J. Liu, Duality between two generalized aubry-andré models with exact mobility edges, *Phys. Rev. B* **103**, 174205 (2021).
 - [69] A. R. Akhmerov, J. P. Dahlhaus, F. Hassler, M. Wimmer, and C. W. J. Beenakker, Quantized conductance at the majorana phase transition in a disordered superconducting wire, *Phys. Rev. Lett.* **106**, 057001 (2011).
 - [70] Supplementary material for details on (I) Detailed analytical derivation of phase boundaries, (II) Additional numerical results for random binary disordered case, and (III) Performance for Single Disorder Realizations.
 - [71] I. Peschel, Calculation of reduced density matrices from

- correlation functions, [Journal of Physics A: Mathematical and General](#) **36**, L205 (2003).
- [72] I. Peschel and V. Eisler, Reduced density matrices and entanglement entropy in free lattice models, [Journal of Physics A: Mathematical and Theoretical](#) **42**, 504003 (2009).
- [73] I. Peschel, Special review: Entanglement in solvable many-particle models, [Brazilian Journal of Physics](#) **42**, 267 (2012).

Supplementary Material: Entanglement entropy as a probe of topological phase transitions

Manish Kumar,¹ Bharadwaj Vedula,¹ Suhas Gangadharaiah,¹ and Auditya Sharma¹

¹Department of Physics, Indian Institute of Science Education and Research, Bhopal, Madhya Pradesh 462066, India

I. ANALYTICAL STUDY USING TRANSFER MATRIX

Let $\psi_{n,A}$ and $\psi_{n,B}$ be the wavefunction amplitudes at the A and B sites of the n^{th} unit cell, respectively. The Schrödinger equation $H\psi = E\psi$ gives the coupled equations:

$$E\psi_{n,A} = t_1\psi_{n,B} + t_2\psi_{n-1,B}, \quad (\text{S1})$$

$$E\psi_{n,B} = t_1\psi_{n,A} + t_2\psi_{n+1,A}. \quad (\text{S2})$$

From Eq. (S2), we express $\psi_{n+1,A}$ as

$$\psi_{n+1,A} = \frac{E\psi_{n,B} - t_1\psi_{n,A}}{t_2}. \quad (\text{S3})$$

Shifting Eq. (S1) by one lattice site,

$$E\psi_{n+1,A} = t_1\psi_{n+1,B} + t_2\psi_{n,B}.$$

Substituting $\psi_{n+1,A}$ from Eq. (S3) into the above gives

$$E \left(\frac{E\psi_{n,B} - t_1\psi_{n,A}}{t_2} \right) = t_1\psi_{n+1,B} + t_2\psi_{n,B}.$$

Rewriting, we obtain

$$\psi_{n+1,B} = -\frac{E}{t_2}\psi_{n,A} + \frac{E^2 - t_2^2}{t_1 t_2}\psi_{n,B}. \quad (\text{S4})$$

Combining Eqs. (S3) and (S4), the dynamics can be expressed in the transfer-matrix form:

$$\begin{pmatrix} \psi_{n+1,A} \\ \psi_{n+1,B} \end{pmatrix} = T_n \begin{pmatrix} \psi_{n,A} \\ \psi_{n,B} \end{pmatrix}, \quad (\text{S5})$$

where the transfer matrix is

$$T_n = \begin{pmatrix} -\frac{t_1}{t_2} & \frac{E}{t_2} \\ -\frac{E}{t_2} & \frac{E^2 - t_2^2}{t_1 t_2} \end{pmatrix}. \quad (\text{S6})$$

For the states at $E = 0$, the transfer matrix reduces to

$$T_n(E = 0) = \begin{pmatrix} -\frac{t_1}{t_2} & 0 \\ 0 & -\frac{t_2}{t_1} \end{pmatrix}. \quad (\text{S7})$$

The Lyapunov exponent associated with the zero-energy modes is defined as

$$\gamma_0 = \lim_{L \rightarrow \infty} \frac{1}{L} \ln \|\mathcal{T}_L\|, \quad (\text{S8})$$

where

$$\mathcal{T}_L = \prod_{n=1}^L T_n \quad (\text{S9})$$

is the total transfer matrix, and $\|\mathcal{T}_L\|$ represents its norm. We take the norm to be the largest absolute eigenvalue of the transfer matrix.

A. Clean SSH model

For the clean SSH model, the hopping terms are given by

$$\begin{aligned} t_1 &= t - \lambda, \\ t_2 &= t + \lambda. \end{aligned} \quad (\text{S10})$$

In this case, since all the transfer matrices T_n are the same, the total transfer matrix is

$$\mathcal{T}_L = \begin{pmatrix} \left(-\frac{t_1}{t_2}\right)^L & 0 \\ 0 & \left(-\frac{t_2}{t_1}\right)^L \end{pmatrix}. \quad (\text{S11})$$

Here we want to calculate the Lyapunov exponent of the edge states. For edge states to appear, the system has to be in the topological regime, i.e. $|t_2| > |t_1|$. Therefore, following Eqs. (S8) and (S9), the LE is

$$\gamma_0 = \lim_{L \rightarrow \infty} \frac{1}{L} \ln \left| \left(\frac{t_2}{t_1} \right)^L \right| = \ln \left| \frac{t_2}{t_1} \right|. \quad (\text{S12})$$

In the topological region $\gamma_0 > 0$ because of the localized nature of the edge states and $\gamma_0 \rightarrow 0$ as we approach the phase boundary. Hence the boundary of the topological phase is

$$\left| \frac{t_2}{t_1} \right| = 1. \quad (\text{S13})$$

Since t_1 and t_2 are given by Eq. (S10), the topological phase boundaries become

$$\lambda = 0, \quad t = 0. \quad (\text{S14})$$

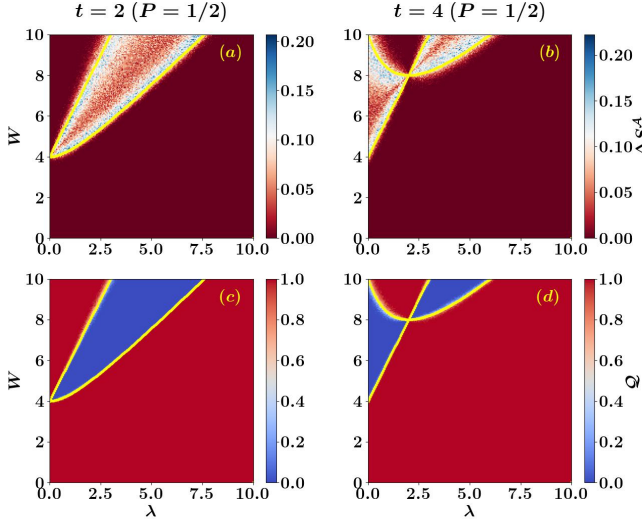


FIG. S1. Phase diagrams for the SSH model with binary disorder with probability $P = 1/2$. (a,b) Entanglement entropy difference $\Delta S^A = |S_{\text{hf}}^A - S_{\text{hf}+1}^A|$ and (c,d) topological quantum number Q , plotted as functions of binary disorder strength W and dimerization λ . Left column (a,c): $t = 2$; right column (b,d): $t = 4$. For ΔS^A , we use system size $N = 400$ and subsystem size $N_A = 50$ at half-filling ($\text{hf} = N/2$). For Q , $N = 2000$. For all the cases, the averaging is done over 100 disorder realizations. Yellow curves denote analytical phase boundaries derived from Lyapunov exponents, separating topological (red) and trivial (blue) phases. The agreement between ΔS^A , Q , and analytical boundaries confirms the robustness of our approach. Red (blue) regions denote $Q = 1$ ($Q = 0$) and $\Delta S^A = 0$ ($\Delta S^A > 0$), corresponding to topological and trivial phases respectively.

B. Quasiperiodic disorder

In the SSH model with quasiperiodic disorder in the hopping term [1], the intercell and the intracell hopping amplitudes are given by

$$\begin{aligned} t_1 &= t - \lambda - \delta \cos(2\pi\beta n + \phi), \\ t_2 &= t + \lambda + \delta \cos(2\pi\beta n + \phi). \end{aligned} \quad (\text{S15})$$

Using equation Eq. (S9), the total transfer matrix is

$$\mathcal{T}_L = \begin{pmatrix} 1/Z & 0 \\ 0 & Z \end{pmatrix}, \quad (\text{S16})$$

where

$$Z = (-1)^L \prod_{n=1}^L \frac{t + \lambda + \delta \cos(2\pi\beta n + \phi)}{t - \lambda - \delta \cos(2\pi\beta n + \phi)}. \quad (\text{S17})$$

Here $|Z| > |1/Z|$, the reason for which will be clear once we obtain the expression for the LE by considering $|Z|$ as the norm of the transfer matrix. From Eqs. (S8) and

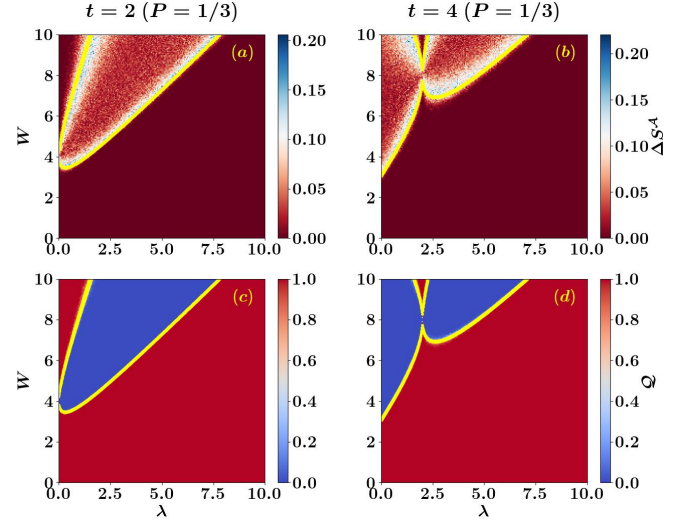


FIG. S2. Phase diagrams for the SSH model with binary disorder with probability $P = 1/3$. The entanglement entropy difference ΔS^A (a,b) and the topological quantum number Q (c,d) are shown as functions of disorder strength W and dimerization λ . Results for two hopping strengths are presented: $t = 2$ (left column) and $t = 4$ (right column). Calculations for ΔS^A are performed on a system of size $N = 400$ with a subsystem of $N_A = 50$ at half-filling, while Q is computed for a larger system ($N = 2000$). Data are averaged over 100 disorder realizations. The analytically derived phase boundaries (yellow curves) excellently match with the numerical results, robustly distinguishing the topological ($Q = 1$, $\Delta S^A = 0$; red) and trivial ($Q = 0$, $\Delta S^A > 0$; blue) phases.

(S9) the LE of the edge states is

$$\gamma_0 = \lim_{L \rightarrow \infty} \frac{1}{L} \ln |Z|, \quad (\text{S18a})$$

$$= \lim_{L \rightarrow \infty} \frac{1}{L} \ln \left| \prod_{n=1}^L \frac{t + \lambda + \delta \cos(2\pi\beta n + \phi)}{t - \lambda - \delta \cos(2\pi\beta n + \phi)} \right|. \quad (\text{S18b})$$

Since β is an irrational number, as n varies, the interval $[0, 2\pi]$ fills uniformly. This follows from Weyl's equidistribution theorem and properties of irrational rotations [2, 3]. Then by using the classical Jensen's formula [4, 5], we can write

$$\begin{aligned} \gamma_0 &= \frac{1}{2\pi} \int_0^{2\pi} \ln \left| \frac{t + \lambda + \delta \cos \theta}{t - \lambda - \delta \cos \theta} \right| d\theta \\ &= \frac{1}{2\pi} \int_0^{2\pi} \ln |t + \lambda + \delta \cos \theta| d\theta \\ &\quad - \frac{1}{2\pi} \int_0^{2\pi} \ln |t - \lambda - \delta \cos \theta| d\theta. \end{aligned}$$

Both integrals are of the form

$$\frac{1}{2\pi} \int_0^{2\pi} \ln |a + b \cos u| du = \begin{cases} \ln \frac{|a| + \sqrt{a^2 - b^2}}{2}, & \text{if } |a| > |b|, \\ \ln \frac{|b|}{2}, & \text{if } |a| < |b|. \end{cases}$$

Using this expression and a careful analysis of the inequalities, the Lyapunov exponent γ_0 for the edge state can be written as

$$\gamma_0 = \begin{cases} \ln \frac{t+\lambda + \sqrt{(t+\lambda)^2 - \delta^2}}{|t-\lambda| + \sqrt{(t-\lambda)^2 - \delta^2}}, & \text{if } \delta < |t-\lambda|, \\ \ln \frac{t+\lambda + \sqrt{(t+\lambda)^2 - \delta^2}}{\delta}, & \text{if } |t-\lambda| < \delta < t+\lambda. \end{cases} \quad (\text{S19})$$

Clearly, $\gamma_0 > 0$ for $\delta < t + \lambda$, indicating localized edge states and hence a topological insulating phase. In contrast, $\gamma_0 \rightarrow 0$ as $\delta \rightarrow t + \lambda$, therefore the topological phase boundary is

$$\delta = t + \lambda. \quad (\text{S20})$$

This analytical expression is consistent with both our numerical results and earlier numerical studies on the SSH model with quasiperiodic modulation in the hopping amplitudes [1].

From Eq. (S16) we can see that the total transfer matrix \mathcal{T}_L has two eigenvalues Z and $1/Z$. The LE obtained in Eq. (S19) is by considering the eigenvalue Z . Hence, a positive value of γ_0 indicates that $|Z| > 1$ (according to Eq. (S18a)), supporting our choice of Z as the largest absolute eigenvalue.

C. Random binary disorder

We consider the disordered SSH model where the hopping terms are given by

$$\begin{aligned} t_1 &= t - \lambda - \Delta_n, \\ t_2 &= t + \lambda + \Delta_n. \end{aligned} \quad (\text{S21})$$

The hopping modulation Δ_n is [6]

$$\Delta_n = \begin{cases} 2, & \text{with probability } P; \\ 2 - W, & \text{with probability } 1 - P. \end{cases} \quad (\text{S22})$$

Here, Δ_n can take only two values for any n , and hence the transfer matrices can take only two possible forms,

$$T_a = \begin{pmatrix} -\frac{v}{u} & 0 \\ 0 & -\frac{u}{v} \end{pmatrix} \quad (\text{S23})$$

corresponding to $\Delta_n = 2$ (with probability P), and

$$T_b = \begin{pmatrix} -\frac{v+W}{u-W} & 0 \\ 0 & -\frac{u-W}{v+W} \end{pmatrix} \quad (\text{S24})$$

corresponding to $\Delta_n = 2 - W$ (with probability $1 - P$), where $u = t + \lambda + 2$ and $v = t - \lambda - 2$. Hence, in Eq. (S9) for the total transfer matrix, T_a appears PL number of times, and T_b appears $(1 - P)L$ number of times in the product. Furthermore, since the transfer matrices T_a and T_b commute in our case, the total transfer matrix can be written as

$$\mathcal{T}_L = T_a^{LP} T_b^{L(1-P)}. \quad (\text{S25})$$

Using Eqs. (S8) and (S9) the LE of the edge states can be written as

$$\gamma_0 = P \ln \|T_a\| + (1 - P) \ln \|T_b\|. \quad (\text{S26})$$

For the edge modes to exist, the intercell hopping has to be larger than the intracell hopping, i.e., $|t_2| > |t_1|$. Therefore, $\|T_a\| = \left| \frac{u}{v} \right|$ and $\|T_b\| = \left| \frac{u-W}{v+W} \right|$. Hence,

$$\begin{aligned} \gamma_0 &= P \ln \left| \frac{u}{v} \right| + (1 - P) \ln \left| \frac{u - W}{v + W} \right| \\ &= \ln \left(\left| \frac{u}{v} \right|^P \left| \frac{u - W}{v + W} \right|^{1-P} \right) \\ &= \ln \left| \left(\frac{u}{v} \right)^P \left(\frac{u - W}{v + W} \right)^{1-P} \right|. \end{aligned} \quad (\text{S27})$$

The phase transition occurs when $\gamma_0 = 0$, thus

$$\left| \left(\frac{u}{v} \right)^P \cdot \left(\frac{u - W}{v + W} \right)^{1-P} \right| = 1. \quad (\text{S28})$$

Note that $u > 0$ for $t, \lambda > 0$. However, v can be negative as well as positive. For $v > 0$,

$$W_{\pm} = \frac{u^{\frac{1}{1-P}} \mp v^{\frac{1}{1-P}}}{u^{\frac{P}{1-P}} \pm v^{\frac{P}{1-P}}}, \quad (\text{S29})$$

and for $v < 0$,

$$W_{\pm} = \frac{u^{\frac{1}{1-P}} \mp (-v)^{\frac{1}{1-P}}}{u^{\frac{P}{1-P}} \mp (-v)^{\frac{P}{1-P}}}. \quad (\text{S30})$$

These equations yield the boundaries separating the topological insulator phase from the trivial insulator phase.

II. ADDITIONAL RESULTS FOR RANDOM BINARY DISORDER CASE

Here we present our numerical results for the SSH model with random binary disorder in the hopping amplitudes. We first show the plots with probability $P = 1/2$ for various values of t . The topological phase is clearly distinguished from the trivial phase in the W - λ plane, as shown by the entanglement entropy difference ΔS^A in Figs. S1(a)-(b), and by the topological invariant Q

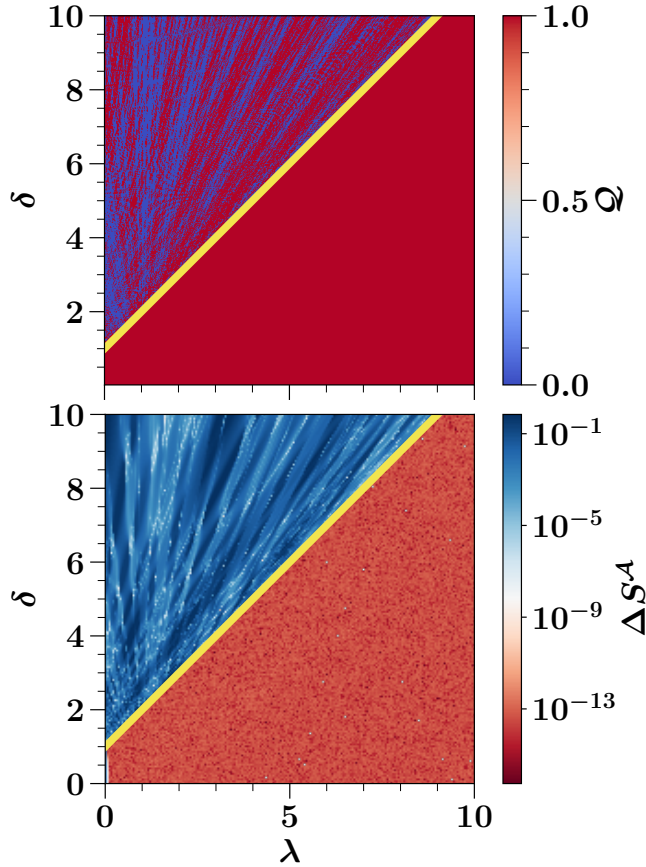


FIG. S3. Comparative phase diagrams for a single realization of quasiperiodic disorder. (a) Phase diagram computed from the topological quantum number \mathcal{Q} ($N = 2000$). The topological phase ($\delta < t + \lambda$) is correctly identified ($\mathcal{Q} = 1$, red). However, \mathcal{Q} also yields a value of 1 in several patches deep inside the trivial phase ($\delta > t + \lambda$), indicating a lack of reliability for single configurations. (b) Phase diagram computed from the entanglement entropy difference $\Delta S^A = |S_{\text{hf}}^A - S_{\text{hf}+1}^A|$ ($N = 400$). The distinction between phases is unambiguous: ΔS^A remains of the order of 10^{-13} (effectively zero, red) within the topological phase and rises to values greater than 10^{-5} (blue) in the trivial phase. The analytical phase boundary $\delta = t + \lambda$ is shown in yellow. While Fig. 2(c) and 2(f) in the main paper shows data for fix λ for varying δ , here we show the entire phase diagram.

in Figs. S1(c)-(d), thereby confirming the consistency of our numerical technique. Additionally, the yellow curves represent the analytically obtained phase boundaries, which cleanly separates the topological and trivial

phases, thereby validating our analytical method.

Next, we examine the case of $P = 1/3$. In this scenario, the disorder Δ_n is distributed as:

$$\Delta_n = \begin{cases} 2, & \text{with probability } 1/3, \\ 2 - W, & \text{with probability } 2/3. \end{cases} \quad (\text{S31})$$

The analytical expressions for the topological phase boundaries are obtained by substituting $P = 1/3$ into Eq. (S29) and Eq. (S30). We validate these boundaries numerically using both the entanglement entropy difference ΔS^A and the topological invariant \mathcal{Q} , as shown in Fig. S2. The excellent agreement between the analytical and numerical results further confirms the robustness of our approach.

III. PERFORMANCE FOR SINGLE DISORDER REALIZATIONS

The efficacy of a topological diagnostic must be evaluated not only after statistical averaging but also for individual disorder configurations. We assess this by comparing the topological quantum number \mathcal{Q} and the entanglement entropy difference ΔS^A for a fixed value of the quasiperiodic phase ϕ .

Figure S3(a) displays the phase diagram determined by \mathcal{Q} for a single disorder realization. The method correctly assigns $\mathcal{Q} = 1$ to the entire topological phase ($\delta < t + \lambda$), as defined by the analytical boundary. However, its utility for a single sample is limited by its performance in the trivial regime ($\delta > t + \lambda$), where it frequently also returns a value of $\mathcal{Q} = 1$. This results in a phase diagram with extensive patches incorrectly identified as topological, demonstrating that \mathcal{Q} may not be a robust diagnostic in the presence of disorder.

The behavior of ΔS^A , shown in Fig. S3(b), is markedly different and more definitive. In the topological phase, ΔS^A assumes values of the order of 10^{-13} , which is numerically equivalent to zero within machine precision. Upon crossing into the trivial phase, it jumps by several orders of magnitude to values greater than 10^{-5} . This sharp, discontinuous change coincides precisely with the theoretical boundary $\delta = t + \lambda$. Consequently, ΔS^A provides a clear and unambiguous binary indicator of the phase for any given parameter set (δ, λ) , even for a single disorder realization. This property highlights a significant practical advantage of the entanglement-based measure over the topological quantum number \mathcal{Q} .

-
- [1] T. Liu and H. Guo, Topological phase transition in the quasiperiodic disordered su-schrier-heeger chain, *Physics Letters A* **382**, 3287 (2018).
 - [2] H. Weyl, Über die gleichverteilung von zahlen mod. eins, *Mathematische Annalen* **77**, 313 (1916).

- [3] G. H. Choe, Ergodicity and irrational rotations, *Proceedings of the Royal Irish Academy. Section A: Mathematical and Physical Sciences* **93A**, 193 (1993).
- [4] S. Longhi, Metal-insulator phase transition in a non-hermitian aubry-andré-harper model, *Phys. Rev. B* **100**, 125157 (2019).

- [5] I. S. Gradshteyn and I. M. Ryzhik, *Table of Integrals, Series, and Products*, seventh ed., edited by D. Zwillinger (Academic Press, Amsterdam, 2007).
- [6] S.-N. Liu, G.-Q. Zhang, L.-Z. Tang, and D.-W. Zhang, Topological anderson insulators induced by random binary disorders, [Physics Letters A **431**, 128004 \(2022\)](#).
- [7] I. C. Fulga, F. Hassler, A. R. Akhmerov, and C. W. J. Beenakker, Scattering formula for the topological quantum number of a disordered multimode wire, [Phys. Rev. B **83**, 155429 \(2011\)](#).
- [8] P. Zhang and F. Nori, Majorana bound states in a disordered quantum dot chain, [New Journal of Physics **18**, 043033 \(2016\)](#).
- [9] A. R. Akhmerov, J. P. Dahlhaus, F. Hassler, M. Wimmer, and C. W. J. Beenakker, Quantized conductance at the majorana phase transition in a disordered superconducting wire, [Phys. Rev. Lett. **106**, 057001 \(2011\)](#).